To Appear in Astrophysical Journal

On the Interferometric Sizes of Young Stellar Objects

J. D. Monnier and R. Millan-Gabet

Harvard-Smithsonian Center for Astrophysics, 60 Garden Street, Cambridge, MA, 02138

jmonnier@cfa.harvard.edu, rmillan@cfa.harvard.edu

ABSTRACT

Long-baseline optical interferometers can now detect and resolve hot dust emission thought to arise at the inner edge of circumstellar disks around young stellar objects (YSOs). We argue that the near-infrared sizes being measured are closely related to the radius at which dust is sublimated by the stellar radiation field. We consider how realistic dust optical properties and gas opacity dramatically affect the predicted location of this dust destruction radius, an exercise routinely done in other contexts but so far neglected in the analysis of near-infrared sizes of YSOs. We also present the accumulated literature of near-infrared YSO sizes in the form of a "size-luminosity diagram" and compare with theoretical expectations. We find evidence that large ($\gtrsim$1.0 μm) dust grains predominate in the inner disks of T Tauri and Herbig Ae/Be stars, under the assumption that the inner-most gaseous disks are optically-thin at visible wavelengths.

Subject headings: accretion disks — radiative transfer — instrumentation: interferometers — circumstellar matter — stars: pre-main sequence — stars: formation

1. Introduction

Radically improved infrared (IR) detectors (Millan-Gabet et al. 1999a) have recently allowed optical interferometers to investigate the inner accretion disks around young stellar objects (YSOs) for the first time (Malbet et al. 1998; Millan-Gabet et al. 1999b; Millan-Gabet 1999; Akeson et al. 2000; Millan-Gabet et al. 2001; Tuthill et al. 2001; Danchi et al. 2001; Akeson et al. 2002). In most cases, the near-IR sizes were found to be significantly larger than expected from the favored disk models of the time (Malbet & Bertout 1991; Hillenbrand et al. 1992; Hartmann et al. 1993; Chiang & Goldreich 1997).

These modeling efforts typically did not directly consider the near-IR disk sizes; indeed, much of the model sophistication was directed toward explaining the observed long-wavelength ($\lambda\gtrsim10\mu$m) spectral energy distributions. Theoretical work has recently been focused again on reproducing the near-IR properties of YSOs, both the near-IR spectrum and characteristic sizes (Natta et al. 2001;

Dullemond et al. 2001). The new models abandon the optically-thick, spatially-thin gas disk in the inner-most region, incorporating an *optically-thin* central cavity to explain the "large" near-IR sizes (as suggested by Tuthill et al. 2001). Alternatively, some workers argue for a quasi-spherical envelope of dust grains around Herbig Ae/Be stars which also can explain the large characteristic sizes (Miroshnichenko et al. 1997, 1999).

This paper takes a step back from the increasingly complicated models one encounters in the literature in order to develop a minimalist framework useful for interpreting the new interferometric measurements (e.g., as generic, or *model-independent*, as possible). While the essential physics are gradually being incorporated in sophisticated, self-consistent ("physical") models, theoretical guidance is needed now in crafting and interpreting disk size surveys beginning at the Keck Interferometer and the Very Large Telescope Interferometer. Indeed, most of the free parameters in the physical models do not strongly affect the near-IR sizes and only serve to obsfucate the relevant physics in the context of the recent interferometric measurements.

In this Letter, we explore how basic dust grain properties and gas absorption of the stellar ultraviolet continuum can affect the observed characteristic sizes of YSO disks in the near-IR.

2. Compendium of Characteristic Disk Sizes

2.1. The Sample

We begin by presenting Figure 1, which contains in one plot the complete set of published near-IR (1.6μm and/or 2.2μm) sizes of Herbig Ae/Be and T Tauri disks (excluding the accretion-dominated source FU Ori). The extended "disk" component of each source was fitted with a ring model, further explained and justified below, and the ring radius is reported for each target star. The majority of measurements come from the IOTA interferometer (Millan-Gabet et al. 1999b; Millan-Gabet 1999; Millan-Gabet et al. 2001). The Palomar Testbed Interferometer contributed the T Tauri observations as well as one Herbig size (Akeson et al. 2000, 2002). Lastly, aperture masking at the Keck telescope was used for LkHα 101 and MWC 349 (Tuthill et al. 2001; Danchi et al. 2001). The stellar properties (luminosity, effective temperature, distance, etc.) were taken from the original interferometer papers when possible, unless revised spectral types were reported in Mora et al. (2001, for MWC 614, V1295 Aql, MWC 296).

Since single-baseline interferometers typically only measure characteristic sizes and do not easily produce true images, we must use some model for the brightness distribution when discussing a "size." The first image of the near-IR emission from a nearly face-on YSO was recently published by Tuthill et al. (2001), revealing a thin asymmetric ring of emission (edge-on disks have been observed before, e.g. Koresko 1998). Partly based on this result, we have chosen to represent the interferometer measurements in Figure 1 by simple ring models. That is, the visibility data for each source were fit assuming the dust emission comes from a thin ring centered on the stellar point

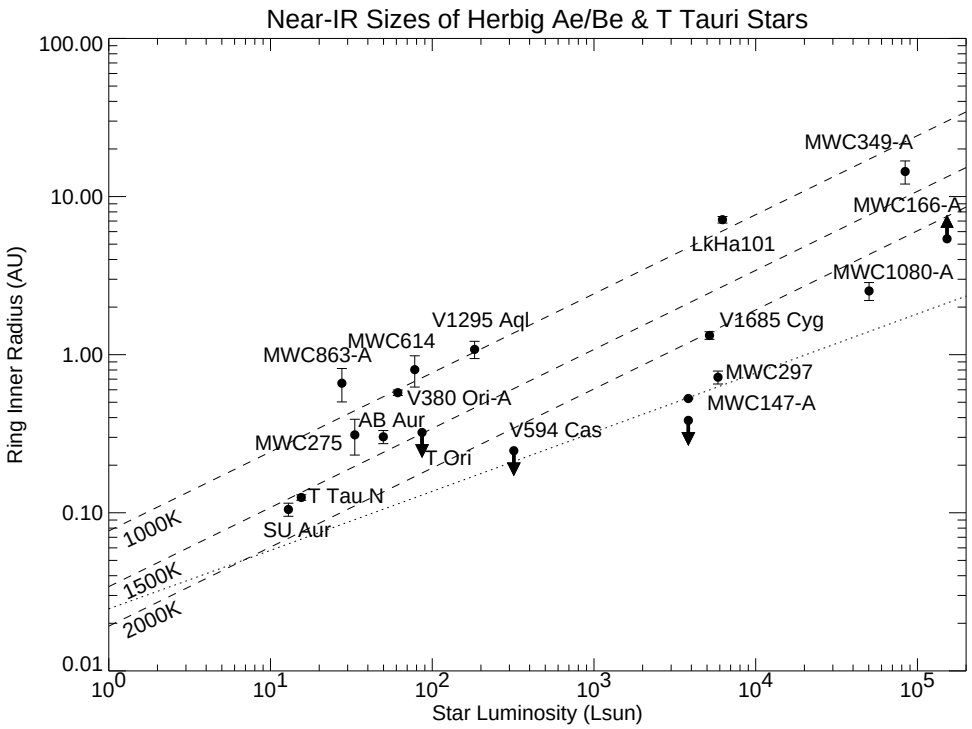

Fig. 1.— This "size-luminosity diagram" is a compendium of all published near-IR disk sizes of YSOs. The plot symbols show the radius of dust emission for the "ring" model discussed in text. The dashed lines represent the expected inner edge of a dust disk truncated by dust sublimation at temperatures T_S =1000 K, 1500 K, and 2000 K, assuming an optically-thin inner cavity and grain absorption efficiency $Q_{\rm abs} = 1$. The dotted line shows the radius of dust destruction (for T_S =1500 K) predicted by the optically-thick, spatially-thin disk model (the "classical" accretion disk) previously held in favor (also $Q_{\rm abs} = 1$).

source (the fraction of light coming from the star was typically estimated by fitting the broad-band spectral energy distribution).

The use of a ring model can also be motivated theoretically. Near-IR ($\lesssim 3\mu$m) dust emission can only come from the hottest dust, and thus only emerges from a narrow range of disk annulii nearest to the star. Further, once the dust opacity becomes $\gtrsim 1$, the inner disk shields the outer disk causing a further drop in dust temperature. While the near-IR "bump" (Hillenbrand et al. 1992) in the spectra of most target sources indicate that the H-band and (especially) K-band fluxes are probably dominated by thermal emission of grains, some fraction of the emission must also be from scattered stellar light. Although scattered light from the inner edge of the disk will not cause a significant change in the observed size, light scattered in a large-scale halo or upper layers of a flared disk could cause the interferometric size to be larger than the disk inner radius, adding a bias toward larger sizes in the size-luminosity diagram (see §4.1 for further discussion)

Different authors implemented the ring model fitting in slightly different ways and we have used the inner ring radii published in the original papers whenever possible (for details, see Millan-

Gabet 1999). This inhomogenity adds only small scatter to the diagram (∼10%) and is insignificant compared to the intrinsic scatter and other sources of uncertainty. The errors bars reflect only the reported uncertainties in the ring radii, and do not include the typically larger uncertainties in the assumed distances and stellar effective temperatures. Note that for early spectral types the temperatures can be uncertain by thousands of Kelvin (e.g. MWC 297 has a 5 spectral subtype uncertainty; Mora et al. 2001). With improved interferometric data, it will become critical to accurately account for these effects and model each source individually.

2.2. Selection Effects

This first generation of YSO disk measurements focused on bright near-IR sources and suffered from some obvious selection effects. The sources typically have unusually large near-IR excesses from thermal emission of hot dust, suggesting that these YSOs could have large disk masses and/or accretion rates (MWC 166 is an exception). The large quantity of hot dust surrounding the sample stars also implies that the inner disks have not yet been cleared of dust, for example by forming planets (e.g. TW Hya, Calvet et al. 2002). Hence, this sample is not designed to study disk evolution, and these disks are all presumably "young." Lastly, the sample will contain few edge-on disks (MWC 349 is an exception, Danchi et al. 2001), since spectra of such sources tend to peak more in the mid-IR (e.g. Lopez et al. 1995).

Interestingly and fortunately, these selection effects do not strongly influence our final conclusions, which ultimately depend most sensitively on the dust grain properties and not the local circumstellar environment.

2.3. Basic Discussion of the "Size-Luminosity Diagram"

From inspection of Figure 1, there is clearly a trend of larger disk inner radii with increasing stellar luminosity L_*, as one would expect if the inner dust disk (or envelope) were truncated by dust evaporation close to the star. In Figure 1 we have also plotted the predicted location of the hottest dust as a function of stellar luminosity for two simple models: an optically-thick, spatially-thin disk model ("classical" accretion disk after Hillenbrand et al. 1992, assuming dust sublimation temperature $T = 1500\,\mathrm{K}$) and a model with an optically-thin inner cavity (radius of dust sublimation $R_s \propto L_*^{\frac{1}{2}}$, after Tuthill et al. 2001, for three different assumed sublimation temperatures T =1000, 1500, 2000 K).

"Classical" accretion disks have a surface temperature $T \propto r^{-\frac{3}{4}}$ since all the heating radiation hits the disk obliquely (Friedjung 1985), the proportionality constant depending on the size and temperature of the star. In order to plot predictions of models which are not functions purely of luminosity, we must relate the stellar properties (e.g, effective temperature) to the luminosity. We have used here an empirical relation fitted to our sample stars, $L_* \propto T_*^{5.3}$, similar to the slope of

the main sequence on the Hertzsprung-Russell diagram. This allows us to plot our size predictions purely as a function of luminosity; the aggregate properties of our sample are sufficient for this Letter but future detailed modeling must take into account the observed stellar properties of each system individually.

As is evident in Figure 1, the classical accretion disk model predictions of the near-IR sizes are too small for nearly every target in our sample. However, the larger sizes predicted by the optically-thin cavity models seem to fit the measurements better (in agreement with the conclusions of Tuthill et al. 2001, for Lkhα 101), although there is large amount of scatter in the diagram for the Herbig Ae/Be stars, as noted by Millan-Gabet et al. (2001). These dust sublimation radii have been estimated as described in detail below, neglecting backwarming by hot grains. One might think that uncertain distances could be a dominant source of scatter in this diagram. However, for a given source, a change in the adopted distance will change both the physical ring inner radius and the stellar luminosity in such a way as to move parallel to the $R_s \propto L_*^{\frac{1}{2}}$ trend lines.

However, we have so far neglected to consider the optical properties of the dust. Tuthill et al. (2001) considered the case of dust sublimating (at temperature T_s) due to heating only by the stellar radiation (neglecting backwarming); the dust sublimation radius R_s follows the standard formula:

$$R_s = \frac{1}{2}\sqrt{Q_R}\left(\frac{T_*}{T_s}\right)^2 R_* = 1.1\,\sqrt{Q_R}\left(\frac{L_*}{1000\,L_\odot}\right)^{\frac{1}{2}}\left(\frac{T_s}{1500\,K}\right)^{-2} AU \qquad (1)$$

where $Q_R = Q_{\rm abs}(T_*)/Q_{\rm abs}(T_s)$ the ratio of the dust absorption efficiencies $Q(T)$ for radiation at color temperature T of the incident and reemitted field respectively.

The dust destruction radius will be increased if one takes into account backwarming by circumstellar dust, a msall correction dependent on the assumed dust distribution. We have also neglected any effects of grains coupling to gas, which can cool through line emission (this would *decrease* the dust destruction radius). However, we are not concerned with second-order effects here and concentrate only on the dominant radiative processes in this Letter.

In the next section we consider how realistic dust properties dramatically affect the predicted location of the dust destruction radius.

3. Effects of Realistic Dust Properties

Many workers have considered how the optical properties of cosmic dust affect our interpretation of astronomical observations (e.g., Draine & Lee 1984, and references therein). A particularly relevant set of papers by Wolfire & Cassinelli (1986, 1987) considered spherically-infalling dust onto a massive protostar. Much of our argument parallels the calculation of these authors (especially at the high-mass limit), although the present application to T Tauri and Herbig Ae/Be stars span sufficiently different physical conditions to justify the specific calculation presented below.

For the goals of this paper, it is sufficient to consider the generic optical properties of representative astronomical dust. For the purpose of calculation we have used the complex dielectric constants of Ossenkopf et al. (1992) for warm astronomical silicates and of Draine & Lee (1984) for graphite. Wavelength- and grain size-dependent absorption efficiencies were calculated assuming spherical grains and Mie scattering theory according to the algorithm of Toon & Ackerman (1981). Most of our discussion will focus on silicate grains, and differences for carbon grains are noted at the end of this section.

Figure 2a shows the absorption efficiency of silicate grains of various sizes as a function of wavelength. The important property to note is that grains emit weakly at wavelengths larger than the grain size. Hence, small grains get heated to higher temperatures for the same impinging radiation because they can not cool efficiently. Also included in this figure are Kurucz models (Kurucz 1979, and subsequent papers) for representative spectral types spanning 1 $L_\odot$ to 10^5 $L_\odot$; note that departures from a Planck function can be significant.

With these results, we can now calculate the factor Q_R in Eq. 1 for various dust sizes. Formally, the dust absorption efficiency for a given grain size a exposed to incident stellar radiation $I_\lambda(T_*)$, is defined as follows: $Q_{\rm abs}(T_*) = \frac{\int Q_{\rm abs}(\lambda) I_\lambda(T_*) d\lambda}{\int I_\lambda(T_*) d\lambda}$. Figure 2b shows the ratio of absorption efficiencies Q_R as a function of stellar effective temperature, assuming an emission temperature of 1500 K (appropriate for dust near sublimation). For large silicate grains ($a \gtrsim 1\ \mu$m), Q_R is relatively insensitive to the stellar effective temperature and close to unity; this is simply because most of the radiation from stars hotter than 3500 K have wavelengths smaller than this grain size. However, the story is radically different for smaller grains. For $a = 0.1\mu$m, Q_R values rise from a value of $\sim$8 for $T_* = 6000K$ to $\sim$50 for $T_* \gtrsim 20000K$. Hence for a hot star, reducing the dust size from 1 μm to 0.1 μm corresponds to nearly a factor of 50 increase in Q_R, resulting in a factor of $\sim$7 increase in dust sublimation radius (see Eq.1).

Figure 3 shows how the dust sublimation radius (for $T_S = 1500K$) changes (compare to Figure 1) using these results for silicate dust grain sizes a=0.1μm and 1.0μm. In creating these curves, we have also assumed that all stellar radiation shortward of 912 Å was scattered away by hydrogen gas in the disk midplane (see §4 for further discussion); this slightly effects the predicted sublimation radius for the only hottest stars.

This figure shows clearly that dust grains with sizes similar to that found in the interstellar medium (0.01μm$< a <$0.25μm, Mathis et al. 1977) would not survive as close to the stars as is observed, assuming $T_s \sim 1500K$. However, larger grains with size $a \gtrsim 1.0\mu$m are able to exist, thus reproducing the sizes observed in Figure 1. This conclusion is more tentative for the T Tauris than for the Herbig stars, due to both the smaller sample size and the less dramatic temperature difference between the photosphere and hot dust. We note that large grains are expected in the midplane of an accretion disk, given that there are sufficient densities and timescales for significant grain growth, even planet formation (e.g., Beckwith & Sargent 1991).

We have also performed these calculations for graphite dust and arrived at the same basic

conclusions. As seen for silicates, it is the grain size that has the strongest effect on Q_R and the near-IR sizes are most consistent with "large" carbon grains ($a \gtrsim 0.3\mu$m). Note that the carbon grains can be somewhat smaller (a factor of 3) than the silicate dust to reproduce the characteristic sizes in Figure 3, due to higher near-IR absorption efficiency.

4. Gas Absorption in the Inner Disk

In Figure 1, we see that disks around the higher luminosity stars tend to be somewhat smaller in size than the lower luminosity sources, compared to the $R_s \propto L_*^{\frac{1}{2}}$ trendline (see Eq. 1). In the last section, we found that realistic dust opacity effects make this discrepancy even greater (see Figure 3).

We suggest that a relatively low-density gas disk in the inner cavity can significantly scatter the ultraviolet continuum from the star, shielding the dust and hence shrinking the near-IR disk sizes. This effect will only occur for hot stars with significant ultraviolet luminosity and could qualititively explain the trend towards under-sized disks for the high luminosity YSOs. Wolfire & Cassinelli (1986) considered a similar effect in calculating the equilibrium temperature structure around an accreting massive protostar. Indeed, Hartmann et al. (1993) showed that the gaseous inner disk of a Herbig Ae/Be star can become optically thick for high accretion rates ($\dot{M} \gtrsim 10^{-7} M_\odot$). But what about at the lower accretion rates currently favored (Hartmann et al. 1993; Gullbring et al. 2000)?

Performing the proper calculation of this effect is beyond the scope of this Letter, however we do consider one limiting case here. We have already eliminated the Lyman continuum photons from the impinging radiation field in creating Figure 3, since neutral H is so efficient at scattering such short wavelengths. From inspection of continuum opacity curves by Novotny (1973), we see that scattering from metals (Si, Fe, Mg) becomes an important opacity source for $\sim$5000 K gas for $\lambda \lesssim 2500$Å. At lower temperatures, molecules can provide an additional source of opacity. In Figure 3, we have plotted additional curves for the dust sublimation radius (R_s) assuming *all the energy* shortward of $\lambda = 2500$Å has been removed from the radiation field, a reasonable limiting case. As expected, this can have strong effects for the hottest stars, $L \gtrsim 1000\, L_\odot$, and should motivate a quantitative study of this effect for realistic inner disk gas models. Ideally, modeling of this curvature in the "size-luminosity" relation will provide a unique and powerful constraint on the density distribution of gas (total column density) of the innermost (dust-free) disk.

We remark on an alternative interpretation of Figure 1 and Figure 2b. The near-IR disk sizes could be explained by a classical accretion disk (optically-thick gas disk in midplane) with *small* ($a \lesssim 0.1\mu$m) grains at the inner radius, where the high Q_R compensates for the loss of stellar energy absorbed/scattered by material in the midplane. However, since the inner gas disk is not expected to be optically-thick for typical T Tauris and Herbig Ae/Be stars, we have not favored this model in this Letter.

4.1. Other Important Effects

Considering the large scatter in the size-luminosity diagram for the Herbig Ae/Be stars (factor of about 3-10 for a given stellar luminosity), there must be additional effects contributing to the observed disk sizes than the grain sizes and gas opacity. Some effects which may be influencing the observed sizes include: additional sources of luminosity (see Hillenbrand et al. 1992; Hartmann et al. 1993), photoevaporation (Hollenbach et al. 1994; Danchi et al. 2001), turbulent accretion (Kuchner & Lecar 2002), or more complicated emission morphology (scattered light, viewing angles, "disk plus envelope" combinations, etc.; Miroshnichenko et al. 1999).

5. Conclusions

Physical models of accretion disks around young stars are critical for understanding the level of IR excess, the spectral energy denstribution, and the interferometric disk sizes. However, such models have a large number of parameters and are subject to many uncertain assumptions. In this Letter we considered only the problem of understanding the observed characteristic near-IR sizes of YSOs. By limiting our focus to just the inner disk, we have motivated a minimalist framework founded on the argument that the characteristic size of a given source is directly related to the radius of dust sublimation.

We investigated quantitatively how the radius of dust sublimation depends on realistic optical constants and gas absorption of the stellar ultraviolet continuum, and we found that the magnitudes of these effects are strong functions of stellar effective temperature and grain size. Our results showed that the observed sizes of YSOs are consistent with the presence of an optically-thin cavity surrounding the star, only if the near-IR emission arises from relatively large dust grains ($a \gtrsim 1 \mu$m for Herbig Ae/Be stars, somewhat smaller grains are allowed for T Tauris) heated to the sublimation temperature ($T_s \sim 1500K$). For the hotter stars (Herbig Be), gas absorption/scattering of the stellar ultraviolet continuum is likely to be non-neglible and may further help explain the observed size-luminosity relations.

Despite success at reproducing the typical sizes, we can not easily explain the large scatter in the size-luminosity diagram for the Herbig Ae/Be stars using this minimalist framework. More complete disk surveys are beginning with the Keck Interferometer and the Very Large Telescope Interferometer to explore these systems in more detail. Further, interferometer arrays, such as IOTA, COAST, and CHARA, image the disk emission from YSOs to determine whether the ring morphology (a central assumption here) is common to these systems or unique to Lkhα 101.

The authors would like to thank many colleagues for discussions and comments: N. Calvet, L. Hartmann, P. Tuthill, J.P. Berger, M. Kuchner, J. Aufdenberg, C. D. Matzner, and A. Natta. This material is based upon work supported by NASA under JPL Contract 1236050 issued through the

Office of Space Science.

REFERENCES

Akeson, R. L., Ciardi, D. R., van Belle, G. T., & Creech-Eakman, M. J. 2002, ApJ, 566, 1124

Akeson, R. L., Ciardi, D. R., van Belle, G. T., Creech-Eakman, M. J., & Lada, E. A. 2000, ApJ, 543, 313

Beckwith, S. V. W. & Sargent, A. I. 1991, ApJ, 381, 250

Calvet, N., D'Alessio, P., Hartmann, L., Wilner, D., Walsh, A., & Sitko, M. 2002, ApJ, 568, 1008

Chiang, E. I. & Goldreich, P. 1997, ApJ, 490, 368

Danchi, W. C., Tuthill, P. G., & Monnier, J. D. 2001, ApJ, 562, 440

Draine, B. T. & Lee, H. M. 1984, ApJ, 285, 89

Dullemond, C. P., Dominik, C., & Natta, A. 2001, ApJ, 560, 957

Friedjung, M. 1985, A&A, 146, 366

Gullbring, E., Calvet, N., Muzerolle, J., & Hartmann, L. 2000, ApJ, 544, 927

Hartmann, L., Kenyon, S. J., & Calvet, N. 1993, ApJ, 407, 219

Hillenbrand, L. A., Strom, S. E., Vrba, F. J., & Keene, J. 1992, ApJ, 397, 613

Hollenbach, D., Johnstone, D., Lizano, S., & Shu, F. 1994, ApJ, 428, 654

Koresko, C. D. 1998, ApJ, 507, L145

Kuchner, M. J. & Lecar, M. 2002, ApJ, 574, L84

Kurucz, R. L. 1979, ApJS, 40, 1

Lopez, B., Mekarnia, D., & Lefevre, J. 1995, A&A, 296, 752

Malbet, F., et al. 1998, ApJ, 507, L149

Malbet, F. & Bertout, C. 1991, ApJ, 383, 814

Mathis, J. S., Rumpl, W., & Nordsieck, K. H. 1977, ApJ, 217, 425

Millan-Gabet, R. 1999, Ph.D. Thesis

Millan-Gabet, R., Schloerb, F. P., & Traub, W. A. 2001, ApJ, 546, 358

Millan-Gabet, R., Schloerb, F. P., Traub, W. A., & Carleton, N. P. 1999a, PASP, 111, 238

Millan-Gabet, R., Schloerb, F. P., Traub, W. A., Malbet, F., Berger, J. P., & Bregman, J. D. 1999b, ApJ, 513, L131

Miroshnichenko, A., Ivezić , Ž., & Elitzur, M. 1997, ApJ, 475, L41

Miroshnichenko, A., Ivezić , Ž., Vinković , D., & Elitzur, M. 1999, ApJ, 520, L115

Mora, A., et al. 2001, A&A, 378, 116

Natta, A., Prusti, T., Neri, R., Wooden, D., Grinin, V. P., & Mannings, V. 2001, A&A, 371, 186

Novotny, E. 1973, Introduction to stellar atmospheres and interiors (New York: Oxford University Press, 1973)

Ossenkopf, V., Henning, T., & Mathis, J. S. 1992, A&A, 261, 567

Toon & Ackerman. 1981, Appl. Opt., 20, 3657

Tuthill, P. G., Monnier, J. D., & Danchi, W. C. 2001, Nature, 409, 1012

Wolfire, M. G. & Cassinelli, J. P. 1986, ApJ, 310, 207

—. 1987, ApJ, 319, 850

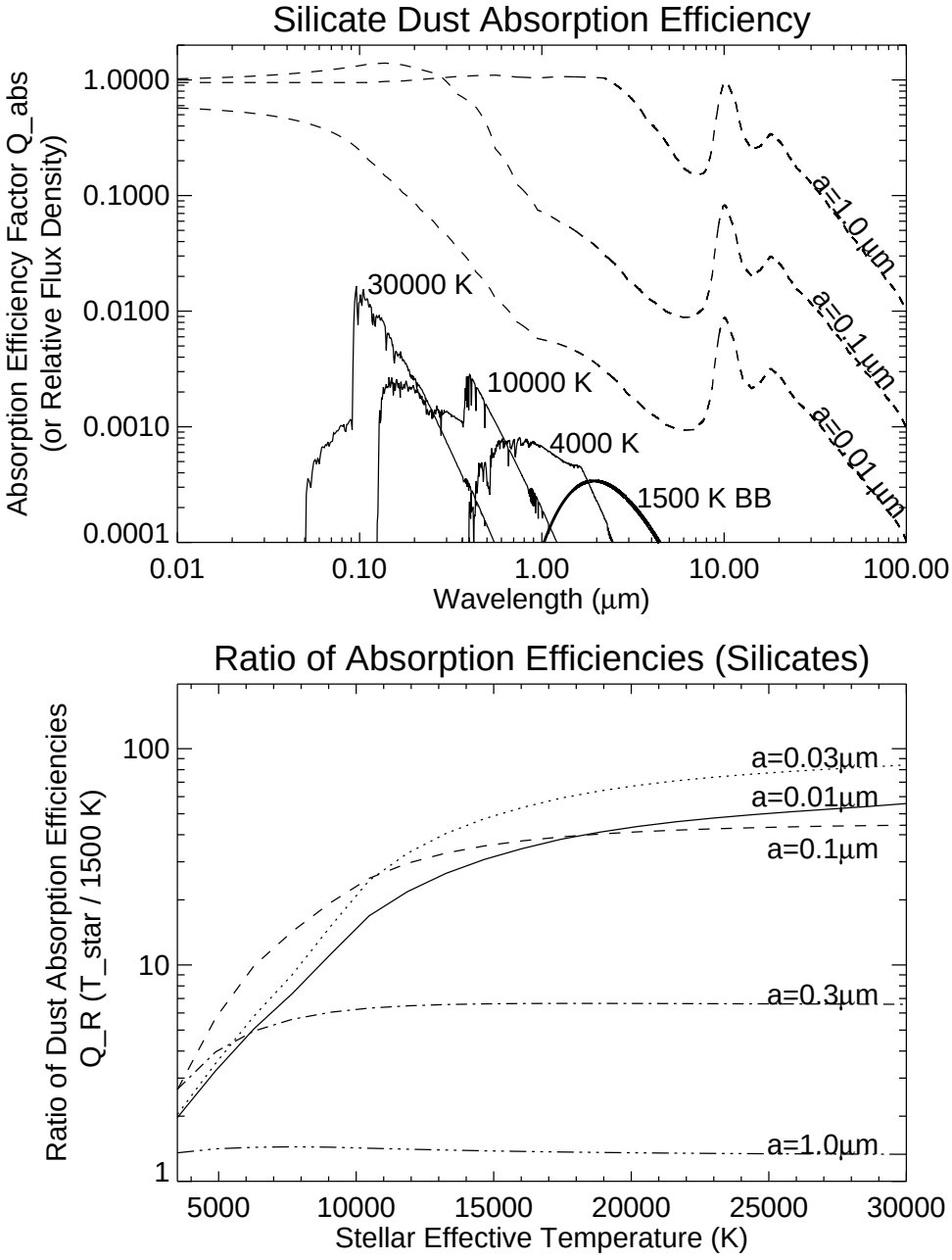

Fig. 2.— *top panel:* a) This figure shows the wavelength-dependent absorption efficiency for silicate dust as a function of dust grain radius a (dashed lines). At the bottom of the plot, Kurucz models (log g 4.1, log Z 0.0) of stars at a range of effective temperatures are plotted (solid lines) to illustrate why the effective dust absorption efficiency is a strong function of spectral type for small grains. *bottom panel:* b) This panel shows the ratio of the dust absorption efficiencies for the incident radiation field versus an assumed 1500 K emission spectrum. See text for mathematical definitions.

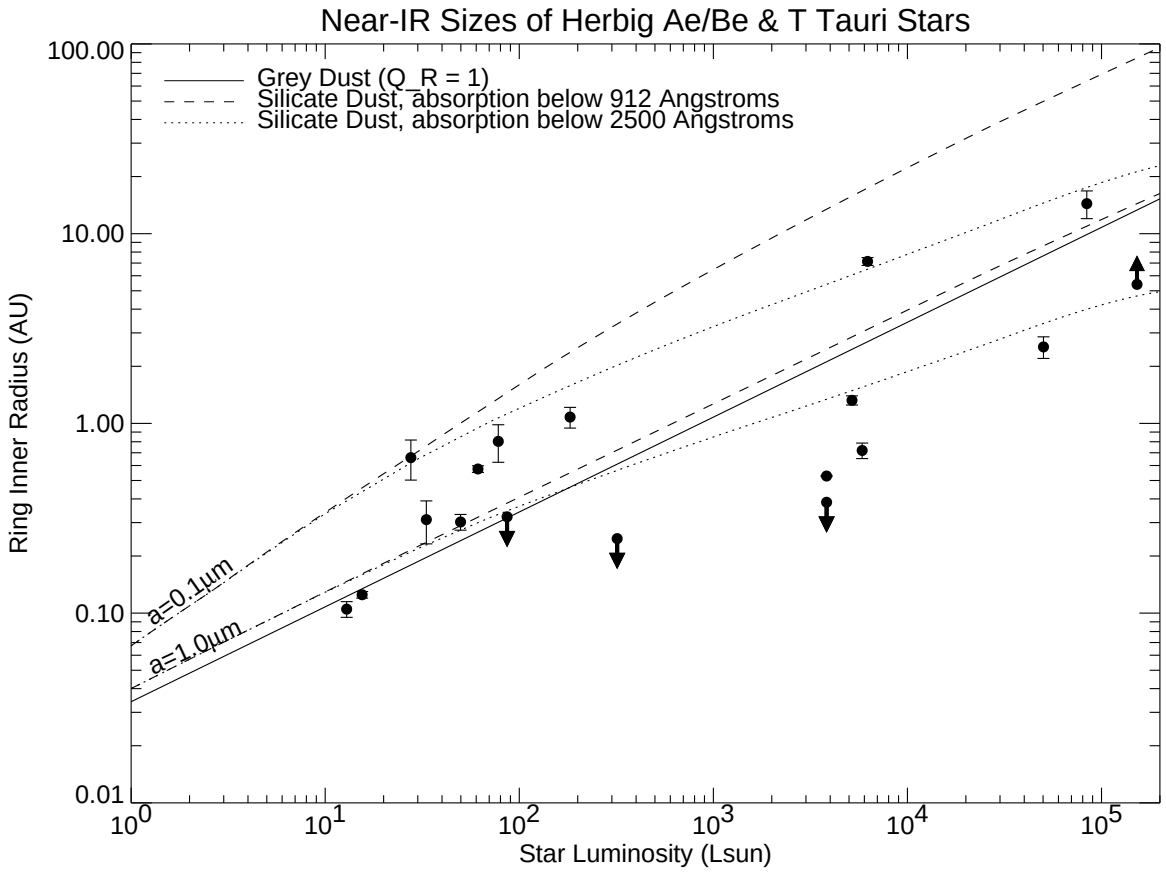

Fig. 3.— This "size-luminosity diagram" illustrates how the predicted disk sizes are modified by taking into account realistic dust opacities and some gas absorption of the UV stellar continuum (all assuming $T_s = 1500K$). The solid line shows radius of dust destruction for grey dust (see $T_S = 1500K$ line in Figure 1). The dashed line assumes the Lyman continuum photons ($\lambda < 912$Å) have all been scattered out of the disk midplane, and the dotted line assumes that the entire UV continuum below $\lambda < 2500$Å has been absorbed before impinging on the dust (see §4 for discussion). Curves for two different grain sizes a are shown.